Title

Tumor Hypomethylation at 6p21.3 Associates with Longer Time to Recurrence of High-Grade Serous Epithelial Ovarian Cancer

Journal

Cancer Research, 74(11)

ISSN

0008-5472

Authors

Wang, Chen
Cicek, Mine S
Charbonneau, Bridget
et al.

Publication Date

2014-06-01

DOI

10.1158/0008-5472.can-13-3198

Peer reviewed

Published OnlineFirst April 11, 2014; DOI: 10.1158/0008-5472.CAN-13-3198

Prevention and Epidemiology

Cancer Research

Tumor Hypomethylation at 6p21.3 Associates with Longer Time to Recurrence of High-Grade Serous Epithelial Ovarian Cancer

Chen Wang[1], Mine S. Cicek[4], Bridget Charbonneau[1], Kimberly R. Kalli[2], Sebastian M. Armasu[1], Melissa C. Larson[1], Gottfried E. Konecny[5], Boris Winterhoff[3], Jian-Bing Fan[6], Marina Bibikova[6], Jeremy Chien[7], Viji Shridhar[4], Matthew S. Block[2], Lynn C. Hartmann[2], Daniel W. Visscher[4], Julie M. Cunningham[4], Keith L. Knutson[9], Brooke L. Fridley[8], and Ellen L. Goode[1]

Abstract

To reveal biologic mechanisms underlying clinical outcome of high-grade serous (HGS) epithelial ovarian carcinomas (EOC), we evaluated the association between tumor epigenetic changes and time to recurrence (TTR). We assessed methylation at approximately 450,000 genome-wide CpGs in tumors of 337 Mayo Clinic (Rochester, MN) patients. Semi-supervised clustering of discovery ($n = 168$) and validation ($n = 169$) sets was used to determine clinically relevant methylation classes. Clustering identified two methylation classes based on 60 informative CpGs, which differed in TTR in the validation set [R vs. L class, $P = 2.9 \times 10^{-3}$, HR = 0.52; 95% confidence interval (CI), 0.34–0.80]. Follow-up analyses considered genome-wide tumor mRNA expression ($n = 104$) and CD8 T-cell infiltration ($n = 89$) in patient subsets. Hypomethylation of CpGs located in 6p21.3 in the R class associated with *cis* upregulation of genes enriched in immune response processes (*TAP1*, *PSMB8*, *PSMB9*, *HLA-DQB1*, *HLA-DQB2*, *HLA-DMA*, and *HLA-DOA*), increased CD8 T-cell tumor infiltration ($P = 7.6 \times 10^{-5}$), and *trans*-regulation of genes in immune-related pathways ($P = 1.6 \times 10^{-32}$). This is the most comprehensive assessment of clinical outcomes with regard to epithelial ovarian carcinoma tumor methylation to date. Collectively, these results suggest that an epigenetically mediated immune response is a predictor of recurrence and, possibly, treatment response for HGS EOC. *Cancer Res; 74(11); 3084–91. ©2014 AACR.*

Introduction

Epithelial ovarian cancer (EOC) represents the fifth most common cause of cancer mortality in women, in part, due to the advanced stage at which patients typically present, with an estimated 22,240 new patients and 14,030 deaths in 2013 in the United States (1). Most deaths (~70%) are among patients who had advanced-stage, high-grade serous (HGS) EOC (2), a histologic subtype shown to have unique tumor epigenetic characteristics (3, 4). The diverse outcomes observed among patients with HGS EOC may relate to different molecular subtypes, even among tumors with similar pathologic characteristics.

Several efforts have been made to characterize genomic features of HGS EOC, including an integrative genomic analysis of The Cancer Genome Atlas (TCGA; ref. 5). However, most prior studies focused on overall survival rather than disease recurrence, had relatively short follow-up time, relied only on tumor mRNA expression information rather than methylation (6, 7), focused only on methylation at selected genes (8–11) or, as in the TCGA, and used an early methylation array of approximately 27,000 CpG sites (5). Thus, although methylation is known to be an essential epigenetic process that can regulate gene expression, resulting in cancer development and spread (12), there is a lack of comprehensive genome-wide studies of DNA methylation and recurrence in HGS EOC.

Here, we investigated the association of genome-wide tumor DNA methylation with HGS EOC time to recurrence (TTR). We performed a methylation semi-supervised clustering analysis and revealed two underlying groups with distinct methylation patterns, which associated with differential outcome. Furthermore, in a subset of patients, we evaluated transcriptome differences between methylation classes, which suggested immune-based mechanistic links to recurrence.

Authors' Affiliations: Departments of [1]Health Sciences Research, [2]Medical Oncology, [3]Obstetrics and Gynecology, and [4]Laboratory Medicine and Pathology, Mayo Clinic, Rochester, Minnesota; [5]Department of Medicine, David Geffen School of Medicine, University of California, Los Angeles; [6]Department of Research, Illumina, San Diego, California; Departments of [7]Cancer Biology and [8]Biostatistics, University of Kansas Medical Center, Kansas City, Kansas; and [9]Vaccine and Gene Therapy Institute of Florida, Port St. Lucie, Florida

Note: Supplementary data for this article are available at Cancer Research Online (http://cancerres.aacrjournals.org/).

C. Wang and M.S. Cicek contributed equally to this work.

Corresponding Author: Ellen L. Goode, Mayo Clinic, 200 First Street SW, Rochester, MN 55905. Phone: 507-266-7997; Fax: 507-266-2478; E-mail: egoode@mayo.edu

doi: 10.1158/0008-5472.CAN-13-3198

Published OnlineFirst April 11, 2014; DOI: 10.1158/0008-5472.CAN-13-3198

Patients and Methods

Study participants

Details on study participants have been described previously (3, 4). Briefly, patients ($n = 337$) were women ages 20 years or above ascertained between 1992 and 2009 at the Mayo Clinic (Rochester, MN) within one year of diagnosis with pathologically confirmed primary invasive HGS EOC. Histology and grade were confirmed by a gynecologic pathologist (D.W. Visscher) who also reviewed tissues to ensure 70% tumor content. Recurrence and vital status were obtained from electronic medical records and the Mayo Clinic Tumor Registry. TTR was defined as time from diagnosis to (i) initiation of second-line therapy or (ii) death, censoring at 10 years; 221 recurrences and an additional 12 deaths (total of 233 recurrences or deaths) were observed. Patients provided informed consent for protocols approved by the Mayo Clinic Institutional Review Board.

Methylation arrays

Methylation measurements were generated on pretreatment fresh-frozen tumors using the Illumina Infinium HumanMethylation450 BeadChip, following the manufacture's protocol (3), interrogating genome-wide CpG sites with more than 485,000 methylation probes (13). Pyrosequencing validation showed satisfactory Pearson correlations with BeadChip data (0.84–0.87; ref. 3). Arrays were processed in three batches: (i) Batch 1 with 121 patients, (ii) Batch 2 with 103 patients, and (iii) Batch 3 with 113 patients. For each batch, we assessed "plate" and "chip within plate" effects through principal component analyses; within each batch, we observed a plate effect. Thus, we normalized for this batch effect by fitting a linear model with fixed plate effect for each logit-transformed CpG probe. The logit-transformed probe mean was added back onto the unstandardized residuals from the model before transforming the values back to the original scale (0 to 1). In addition to these technical artifacts, we also observed a batch effect across Batches 1, 2, and 3. To correct for this artifact we used the same methodology used for the correction of plate and chip effects (3). All adjustments were completed for each CpG probe individual, thus allowing the two different methylation probes (Infinium I and II probes) to have different correction factors. Other approaches for normalization commonly used are the adjustment of probe specific biases by fitting two separate models, a model based on fit to all the Infinium I probes and a second model fit to all the Infinium II probes, or a recently proposed method proposed based on a beta mixture quantile dilation approach (14). Methylation probes were excluded from analysis based on the following criteria: (i) were at the same location as a single-nucleotide polymorphism (dbSNP build 137), (ii) high β-values in bisulfite modification-negative controls (beyond four SDs of mean), and (iii) were detected in <70% of samples (based on a detection P value threshold of 0.05). A total of 442,068, 441,775, and 448,543 Illumina probes passed quality control in Batch 1, Batch 2, and Batch 3, respectively. A total of 440,643 probes common among the three batches were retained for the final analysis, corresponding to 90.7% of the total number of probes (485,577). The intraclass correlation for β-values among CEPH replicates was >0.99 in all three batches and that for tumor duplicate samples was >0.99 in Batch 1 and Batch 2. The intraclass correlation for β-values for tumor duplicate samples between Batch 3 and Batch or Batch 2 was >0.83. Within each batch, we removed samples from analysis for the following reasons: (i) failed bisulfite conversion, (ii) had <92% detected probes, where 92% were based on empirical data, and (iii) cases who had received neoadjuvant chemotherapy. After sample quality control, 337 were retained for statistical analysis. More details of quality control procedures can be obtained in a previous publication (3).

Semi-supervised methylation clustering

Patients were randomly assigned into two collections representing a discovery set ($n = 168$) and a validation set ($n = 169$; Supplementary Table S1). To reveal a methylation signature associated with recurrence risk, a semi-supervised recursive partitioning mixture model (SS-RPMM; ref. 15) was applied to logit-transformed normalized methylation β-values (Supplementary Fig. S1). The "semi-supervised" aspect of the analysis was to perform clustering according to a core set of CpG loci, methylation levels of which were significantly associated with TTR. Using the discovery set, CpG loci were ranked according to their strength of association with recurrence based on Cox modeling of TTR and logit-transformed methylation at each CpG locus separately, allowing for left truncation, adjusting for known prognostic factors, including age, stage, grade, ascites, and surgical debulking status, and right censoring at 10 years. The optimal number of CpG loci (M) for subsequent clustering analysis was determined according to a nested cross-validation procedure. Clustering solution was achieved using RPMM, a hierarchical model-based method for clustering that has been extensively used to cluster array-based methylation data (15, 16). On the basis of the RPMM fit to the discovery set, a probabilistic naïve Bayes classifier was used to predict methylation class membership for the patients in the validation set. Then, patients were assigned to the class with the highest membership probability.

Methylation-expression association

Tumor mRNA expression measurements were profiled on a subset of 104 patients using Agilent Whole Human Genome 4×44K expression arrays; details of these experiments have been reported (3, 17). For each of the M CpG loci selected above, *cis* analyses were performed whereby methylation was associated with expression at each probe within 200 kb using Spearman rank correlations; a total of 973 *cis* methylation-expression associations were evaluated.

Prediction analysis of microarray analysis

A classification method, prediction analysis of microarray (PAM; ref. 18), was used to identify *trans*-genes whose transcriptional levels associated with methylation classes resulting from the clustering described above. The PAM method used the nearest shrunken centroid method to prioritize genes showing large between-methylation-class expression difference and small within-methylation-class variability, through an adjustable shrinkage factor parameter. For each possible value of the shrinkage factor, a 10-fold cross-validation was repeated ten times to compute classification accuracy of

Published OnlineFirst April 11, 2014; DOI: 10.1158/0008-5472.CAN-13-3198

Table 1. Univariate and multivariate analysis of recurrence time in the validation set

	Validation set patients ($N = 169$)			Validation set patients who received both platinum and taxane treatment ($N = 130$)		
Univariate analysis	**HR**	**95% CI**	***P***	**HR**	**95% CI**	***P***
R class	0.50	(0.34–0.74)	5.38×10^{-4}	0.39	(0.26–0.60)	1.20×10^{-5}
Multivariate analysis						
R class	0.52	(0.34–0.80)	2.86×10^{-3}	0.38	(0.24–0.61)	5.38×10^{-5}
Age (continuous)	0.99	(0.97–1.00)	0.25	1.00	(0.98–1.02)	0.71
Stage IV	1.14	(0.71–1.84)	0.58	1.21	(0.73–1.98)	0.46
Grade 4	1.18	(0.76–1.83)	0.46	1.29	(0.79–2.09)	0.31
Ascites (no)	0.37	(0.20–0.69)	1.59×10^{-3}	0.36	(0.19–0.68)	1.55×10^{-3}
Debulking (suboptimal)	1.59	(0.98–2.60)	0.06	1.49	(0.86–2.59)	0.15

NOTE: Because of the small number of stage I and II patients ($n = 10$), these were combined with the stage III referent group to avoid numerical instability of multivariate regression.

resulted gene signature. The optimal shrinkage factor of PAM was chosen according to the highest classification accuracy, and differentially expressed genes were considered to represent a transcriptome signature of each methylation class. These analyses used 104 patients with array-based fresh-frozen tumor RNA expression data.

Immunohistochemistry

Tissue microarrays (TMA) were constructed from 546 tumors using three representative 0.6 mm tumor cores of formalin-fixed paraffin-embedded tissue (tumor area identified by D.W. Visscher), and a subset of these tumors ($n = 89$) were also evaluated using methylation arrays. TMAs were stained with mouse anti-human CD8 monoclonal antibody (Dako). The number of epithelial cells potentially interacting with CD8 T cells was estimated by assigning an infiltration score based on the approximate percentage (0%–10%, 11%–50%, and 50%–100%) of tumor epithelial cells directly adjacent to infiltrating CD8-positive cells (including intraepithelial and tumor-stromal interface). The highest expression among the three cores per patient was used for analysis. The percent agreement in 18% of the cores scored by both the primary scorer and pathologist (D.W. Visscher) was 85%.

Ingenuity functional enrichment and network analysis

To gain additional biologic insight, genes differentially expressed by methylation class were investigated using Ingenuity Pathway Analysis (Ingenuity Systems, www.ingenuity.com) for functional enrichment analysis according to canonical pathways and biologic processes.

Results

Clinical characteristics of the HGS EOC tumors ($n = 337$) examined in two sets, including a discovery set ($n = 168$) and validation set ($n = 169$), are presented in Supplementary Table S1. Using a semi-supervised clustering approach (Supplementary Fig. S1), two TTR-associated methylation classes were derived in the discovery set, referred as right (R) and left (L) classes, the separation of which is determined by an optimal $M = 60$ CpG loci selected by cross-validation. Patients in the R methylation class of the discovery set showed longer TTR as compared with the L class. These 60 CpG loci (Supplementary Table S2) prioritized from the discovery set constitute a methylation signature differentiating patients on their risk of recurrence. None of these loci have been found to have probe cross-hybridization issues (19).

The 60 discriminatory CpGs and the corresponding SSRPMM solution were utilized to predict methylation clusters in the independent validation set. Of 169 patients in the validation set, 94 were assigned to R class, which showed a significantly lower recurrence risk than the L class using either univariate [$P = 5.40 \times 10^{-4}$, HR = 0.50; 95% confidence interval (CI), 0.34–0.74] or multivariate analysis ($P = 2.94 \times 10^{-3}$, HR = 0·52; 95% CI, 0.34–0.80; Table 1; Fig. 1A). In further evaluation, we subset to 130 validation patients who have received both platinum and taxane treatment and repeated univariate and multivariate analysis, leading to a more statistically significant association between methylation cluster and TTR ($P = 1.2 \times 10^{-5}$, HR = 0.39; 95% CI, 0.30–0.60) or ($P = 5.38 \times 10^{-5}$, HR = 0.38; 95% CI, 0.20–0.60), respectively (Table 1; Fig. 1B).

By visualizing methylation patterns in the R and L methylation classes at the 60 loci for the discovery and validation sets (Supplementary Fig. S2), it can clearly be observed that the differential methylation between R and L classes is well conserved from discovery to validation set. This suggests good measurement robustness of the selected CpG loci. In addition, we evaluated relationships between the 60 CpG loci using pairwise correlation (Fig. 2). Correlations included a small "block" of strong positive CpG correlation that had generally negative correlation with other loci; this was also consistent across discovery and validation sets. The block consisted of six adjacent CpG loci on chromosome 6p within the *TAP1* [transporter 1, ATP-binding cassette, subfamily B (MDR/TAP)] gene region. These CpG loci are hypermethylated in the L class compared with the R class, suggesting that a hypermethylation event close to *TAP1* promoter region associates with shorter TTR.

Published OnlineFirst April 11, 2014; DOI: 10.1158/0008-5472.CAN-13-3198

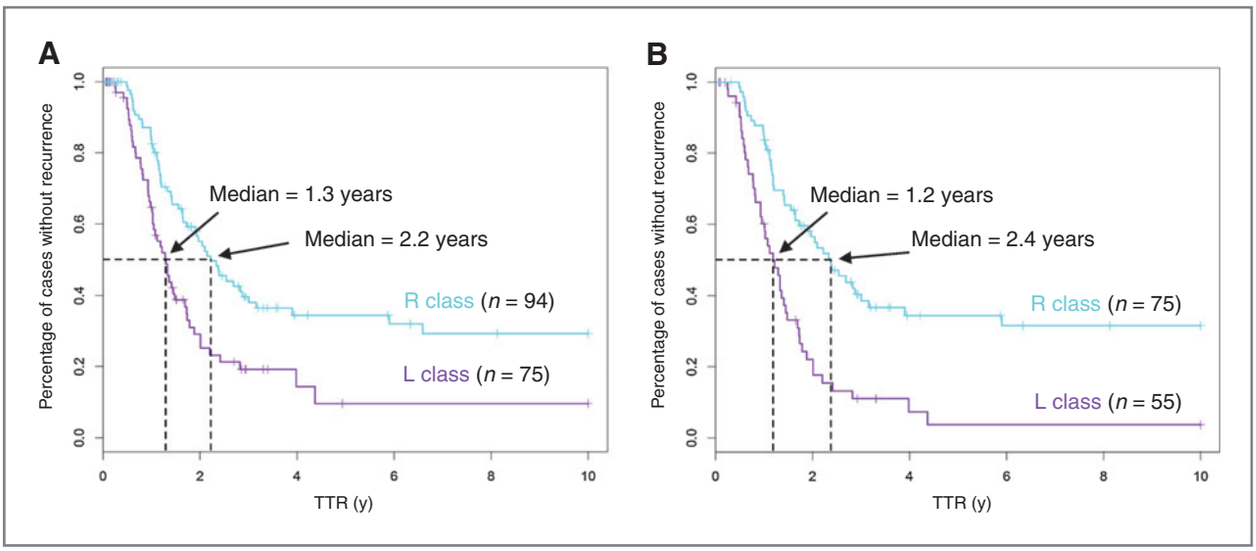

Figure 1. TTR Kaplan–Meier plots. A, for all the patients in validation set ($n = 169$), Kaplan–Meier plot of recurrence time demonstrates a clear outcome difference between R and L methylation classes (univariate analysis $P = 5.38 \times 10^{-4}$), with better outcome in R class. B, for all the validation set patients who received platinum and taxane treatment ($n = 130$), Kaplan–Meier plot of recurrence time shows a stronger outcome difference although still consistent with results using all of patients (univariate analysis $P = 1.20 \times 10^{-5}$). Cyan and purple colors indicate recurrence curves of R and L classes, respectively.

To shed some light on transcriptomic impacts of methylation at the 60 discriminatory CpG loci, we investigated associations between methylation value of these loci and tumor mRNA expression using a subset of patients ($n = 104$). We first focused on *cis* association between methylation and expression of the contiguous structural genes, using a 200-kb window around each CpG locus. Noticeably, chromosome 6 was enriched for significant methylation-expression associations with a greater number of associations between multiple CpG loci on chromosome 6 and *TAP1* gene expression than expected by chance ($P < 2.2 \times 10^{-16}$; Supplementary Table S3 and Supplementary Fig. S3). In the same region, methylation values were also negatively correlated with expression levels of several other genes: *PSMB9, HLA-DQB1, HLA-DQB2*, and *HLA-DMA*. This may suggest that the methylation status of this region influences TTR through regulation of the expression of nearby genes.

Proteins encoded by *TAP1*, *PSMB8*, and *PSMB9* are involved in antigen processing and loading into the human leukocyte antigen (HLA) class I complex. This antigen-processing machinery (APM) is expressed by all cell types and allows tumor antigens to be processed and displayed to cytotoxic CD8 T cells. Therefore, loss of expression of these APM-related genes may enable ovarian cancer cells to evade tumor-specific CD8 T cell–mediated immune response (20). To test whether differential methylation in *TAP1* was associated with presence of CD8 T cells in the tumor, we correlated CD8 immunohistochemical staining with methylation in this region among a subset of 89 patients. We indeed found that hypermethylation of *TAP1* (associated with lower expression of *TAP1* transcript) correlated with lower infiltration of CD8 T cells (shown in Fig. 3), with Spearman correlation coefficient $= -0.41$ ($P = 7.62 \times 10^{-5}$). The correlation remains similar but with increased statistical significance (coefficient $= -0.39$, $P = 5.20 \times 10^{-8}$), when 190 patients with CD8 measurements in both discovery and validation sets were accounted for. This result suggests that epigenetic silencing of *TAP1* and concomitant suppression of CD8 T-cell tumor infiltration may underlie HGS EOC TTR.

We also studied *trans*/*distal* associations for the 60 CpG loci of interest using genome-wide expression array measurements ($n = 104$ patients). On the basis of R/L methylation-class assignments, we utilized the PAM classification algorithm (18) to identify a parsimonious list of genes differentially expressed between R and L classes. According to the most accurate classification scheme, we identified 2,337 PAM expression probes mapped to 1,670 unique genes, which were differentially expressed in the R and L classes (Supplementary Table S4). Among these genes, 712 genes were upregulated in the L class, and 958 genes were upregulated in the R class. Specifically, 23 expression probes upregulated in the L class are *cis* to the 60 CpG loci of interest in a nearby 200 kb genomic window. They correspond to 18 unique genes, including *STMN1* (Stathmin, also called oncoprotein 18), a previously reported prognostic marker that increases in expression in metastatic ovarian cancer samples versus nonmetastatic ones (21). A total of 42 expression probes upregulated in the R class are *cis* to the 60 CpG loci and correspond to 25 unique genes; 18 of which locate in 6p21.3, again underscoring the functional and prognostic importance of this region. A global expression clustering map according to methylation classes ($N = 104$) is displayed in Supplementary Fig. S4. Genes upregulated in the R class (with longer TTR) were extremely enriched in immune-related pathways, such as antigen presentation ($P = 1.6 \times 10^{-32}$), cross-talk between dendritic cells and natural killer cells ($P = 2 \times 10^{-24}$), and communication between innate and adaptive immune cells ($P = 5 \times 10^{-24}$). This provides further

Published OnlineFirst April 11, 2014; DOI: 10.1158/0008-5472.CAN-13-3198

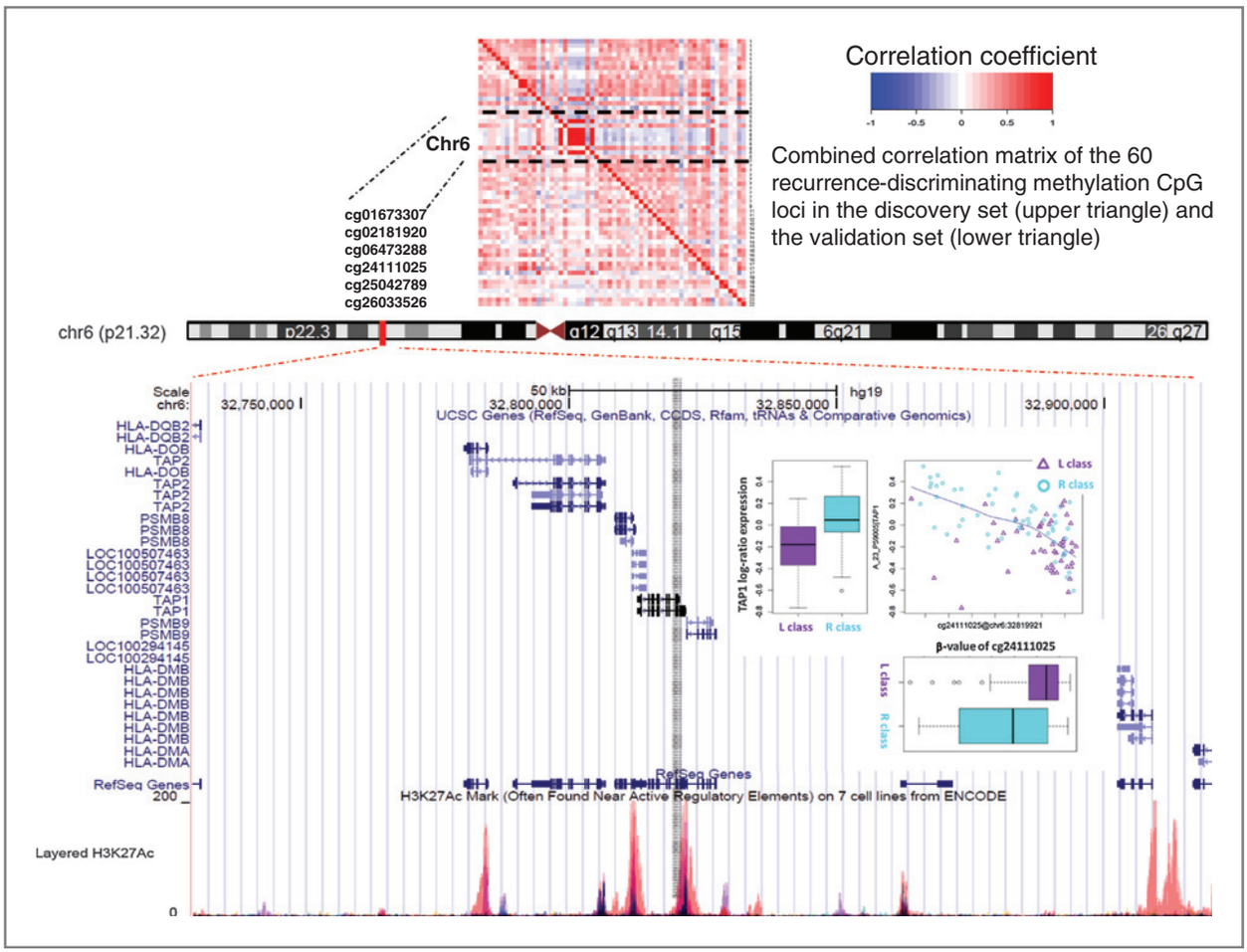

Figure 2. Genomic view of the 6p21.3 region and correlation matrices of 60 selected CpG loci. The top panel shows correlation matrices of methylation at 60 selected CpG loci for discovery set (top) and validation set (bottom). Each column and row of the correlation matrices correspond to one of 60 CpG loci. The bottom panel displays zoom-in UCSC genomic view of 6p21.3, where *TAP1*, *PSMB8*, *PSMB9*, *HLA-DQB1*, *HLA-DQB2*, *HLA-DMA*, and *HLA-DOA* reside. The gene track in the middle is defined according to RefSeq database. The bottom track indicates H3K27Ac marks on seven cell lines from ENCODE project that are often found near regulatory elements. Close to the *TAP1* promoter region, six CpG loci with highly correlated methylation values are highlighted by a gray bar. Insets provide box-plots of *TAP1* CpG cg24111025 methylation by R and L class in the validation set, and TAP1 expression probe A_23_P59005 by R and L class in 104 validation set patients. A representative methylation-expression association is demonstrated in a scatter plot of methylation β-values and expression levels (*TAP1* CpG cg24111025 and TAP1 expression probe A_23_P59005) among 104 patients with HGS EOC in the bottom left.

support for an immune mechanism contributing to the longer TTR we observed in patients with HGS EOC in the R methylation class, supporting the association of antitumor immune responses with improved outcome in other studies (22–25). Detailed pathway enrichment results for L and R class upregulated genes are provided as Supplementary Tables S5 and S6.

Discussion

In this large genome-wide epigenetic study of fresh-frozen tumors, we investigated the utility of DNA methylation to define HGS EOC patient classes with different recurrence times. Our semi-supervised clustering analysis of dense genome-wide DNA methylation data (over 450,000 CpG sites) identified 60 CpG loci in a discovery set ($n = 168$) and replicated in a validation patient set ($n = 169$). Notably, none of these 60 loci were included in the Illumina HumanMethylation27 BeadChip used by the TCGA (5). The prediction of recurrence time by this epigenetic signature was statistically significant in our validation set even after controlling for covariates known to contribute to TTR: age, grade, stage, ascites, and surgical debulking status. In additional transcriptome analysis, we determined that among the two methylation classes (R and L), the R class, which had a longer TTR, showed increased expression of immune-related genes, and reduced methylation at key CpGs correlated with increased CD8 T-cell infiltration, suggesting a more robust immune response.

Evaluation of these epigenetic markers with consideration of other clinical factors revealed additional prognostic value, as shown in Table 1. In multivariate analysis, effective surgical cytoreduction as an established factor affecting recurrence

Published OnlineFirst April 11, 2014; DOI: 10.1158/0008-5472.CAN-13-3198

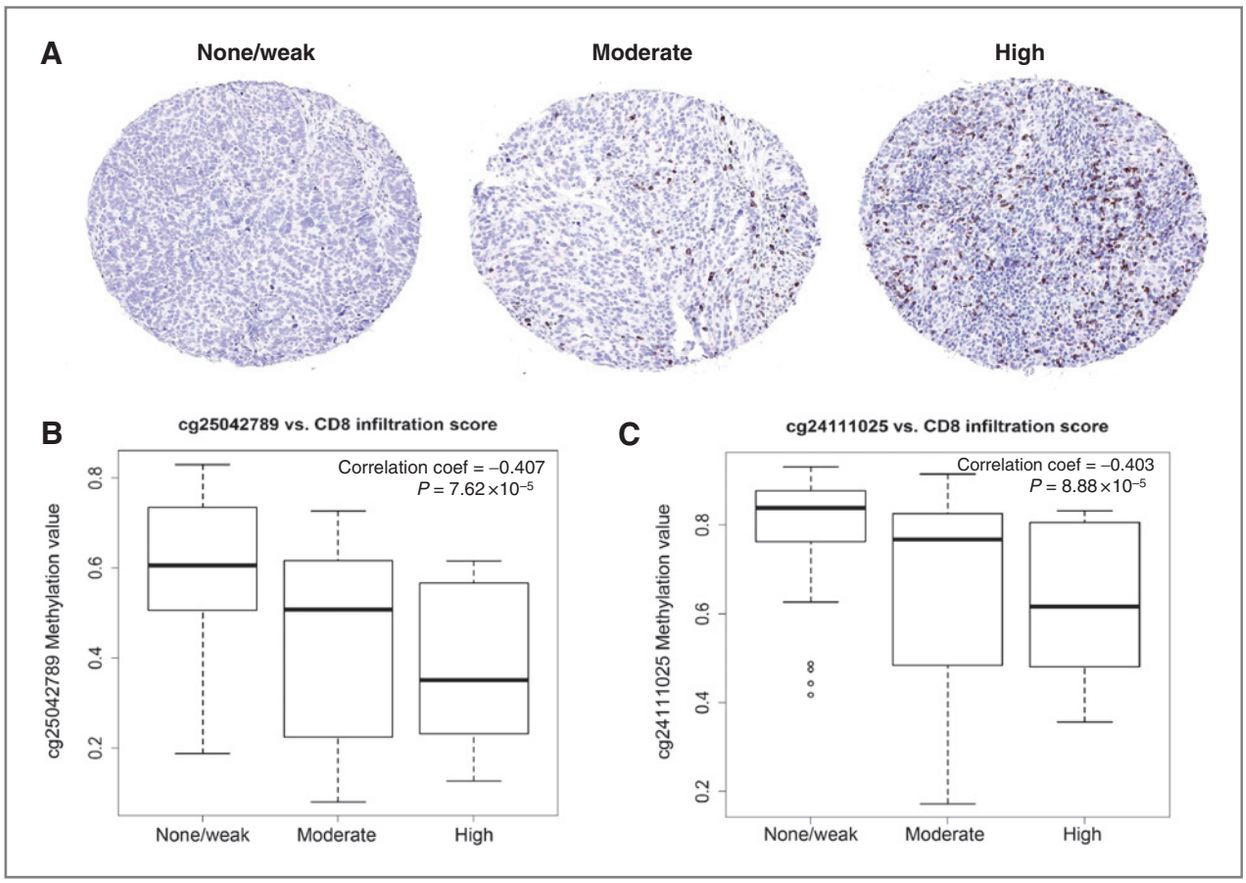

Figure 3. Representative scoring of CD8 immunohistochemistry and its association with TAP1 methylation status. Eighty-nine validation set patients with CD8 scoring results were used to test association with TAP1 methylation status. A, displays representative TMA slides for which we used the following scoring system to approximate percentage of tumor epithelial cells directly adjacent to infiltrating cells (includes intraepithelial and tumor interface): (i) none/few = 0% to 10%, (ii) moderate = 11% to 50%, (iii) high = 51% to 100%. B and C, hypermethylation of *TAP1* correlated with lower infiltration of CD8, using two CpG loci cg25042789 and cg24111025 as examples.

achieved only marginally significant association (suboptimal debulking: $P = 0.06$), possibly due to small number of patients (validation set, $n = 35$) that were not optimally cytoreduced. This confirms the recognition that aggressive surgery, whenever possible, is important to reduce recurrence risk. Another key clinical factor, lack of ascites at surgery, also shows a comparably significant association with superior outcome ($P = 1.55 \times 10^{-3}$), independent of methylation clusters. These multivariate results raise the possibility that known prognostic factors can be combined with epigenetic markers to build more accurate TTR prediction models.

To better understand the downstream functional impacts of differential methylation, we also integrated tumor mRNA expression, and both *cis* and *trans*-integrative analyses suggested immune response as an underlying mechanism. First, *cis* methylation-expression associations within a local genomic window of 200 kb revealed significant downregulation of *TAP1* by methylation. Second, global transcriptome differences investigated by methylation class highlighted biologic processes related to the immune response in the R class with superior outcome. The key finding from this study was that DNA hypermethylation was negatively correlated with gene expression particularly on 6p21.3 ($P < 2.2 \times 10^{-16}$). The genes included in this region were *TAP1*, *PSMB8*, *PSMB9*, *HLA-DQB1*, *HLA-DQB2*, *HLA-DMA*, and *HLA-DOA*.

Several studies have shown some prognostic association with HLA and TAP1 expression in ovarian carcinomas, but most were based on small-scale protein staining methods that relied on subjective scoring (26, 27). Furthermore, for the region of 6p21.3 harboring *TAP1* and several *HLA* genes, we revealed that its hypermethylation status is significantly correlated with lower infiltration of CD8 T cells. Higher numbers of CD8 T cells infiltrating the tumor has previously been reported in association with improved survival in EOC (28).

HLA-DQB1, *HLA-DQB2*, *HLA-DMA*, and *HLA-DOA*, all encode components of the HLA class II complex. This complex is important for presenting antigens to CD4 helper T cells. Unlike HLA class I, which is expressed on the majority of cells, HLA class II expression is generally restricted to professional antigen-presenting cells (APC), namely dendritic cells, macrophages, and B cells. Therefore, this methylation pattern might reflect the presence of APCs in the tumor microenvironment,

Published OnlineFirst April 11, 2014; DOI: 10.1158/0008-5472.CAN-13-3198

as a tumor epithelial cell-predominant (but not pure) sample was used to obtain RNA and DNA for this study. Methylation patterns can reveal cell populations present in the tumor, as demonstrated by Dedeurwaerder and colleagues, who found that outcome-associated methylation patterns in breast cancer were similar to methylation patterns typical of T cells and indicative of T-cell infiltration (29). Alternatively, previous studies have demonstrated aberrant expression of HLA class II components on EOC cells (30, 31). For example, one study by Callahan and colleagues that has parallels to our study, showed that aberrant HLA-DMB expression by ovarian cancer epithelial cells was associated with CD8 T-cell infiltration and a marked improvement in survival (30).

Utilizing genome-wide methylation analysis with gene expression-based follow-up, we have identified hypermethylation in 6p21.3 as a potential cause for downregulation of several genes related to HLA class I and class II antigen presentation in the context of HGS EOC. This suggests a role for immune-mediated tumor killing in the observed TTR differences, as greater antigen presentation should result in a more active immune response to tumors. The additional finding that hypomethylation of these genes is associated with higher CD8 infiltration in the tumors further supports this concept. Discovery of this methylation-mediated mechanism could have meaningful clinical implications, distinguishing patients whose tumors would be most responsive to immunotherapy. In addition, elucidating patients with hypermethylated antigen-processing genes might help identify those who would benefit from immunotherapy combined with adjuvant DNA hypomethylating agents or histone deacetylase inhibitors, as these agents were previously reported to recover HLA and TAP1/2 expression in cervical cancer cell lines, allowing them to be recognized by cytotoxic T cells (32, 33); both are currently in preclinical HGS EOC studies.

Interestingly, downregulation or loss of the TAP1 protein has been reported in high-grade breast cancer (34) and found to be associated with metastasis (35) in breast cancer. Here, we revealed downregulation of *TAP1*, which is largely associated with hypermethylation of several CpG loci within its gene region in HGS EOC. Several genes related to HLA class II antigens have also been found to have significant methylation-expression association in a follow-up analysis (Supplementary Table S2), including HLA-DOA (MHC, class II, DO-α), HLA-DMA (MHC class II, DM-α), and HLA-DQB1 (MHC class II, DQ-β1).

In conclusion, our comprehensive analysis of HGS EOC tumor DNA methylation with respect to disease recurrence revealed the presence of two epigenetic subtypes with significant differences in TTR, even with adjustment for clinical features. The differentiating CpG loci we identified may play an important role in antitumor immunity and may aid in identification of patients who would be good candidates for immunotherapy or who would benefit from combining a DNA hypomethylating agent with immunotherapy.

Disclosure of Potential Conflicts of Interest

B. Charbonneau is employed and has ownership interest in Eli Lilly and Company. No potential conflicts of interest were disclosed by the other authors.

Authors' Contributions

Conception and design: C. Wang, M.S. Cicek, B. Winterhoff, D.W. Visscher, K.L. Knutson, B.L. Fridley, E.L. Goode

Development of methodology: C. Wang, M.S. Cicek, J.-B. Fan, E.L. Goode

Acquisition of data (provided animals, acquired and managed patients, provided facilities, etc.): C. Wang, B. Charbonneau, K.R. Kalli, G.E. Konecny, B. Winterhoff, J.-B. Fan, M. Bibikova, J. Chien, L.C. Hartmann, J.M. Cunningham

Analysis and interpretation of data (e.g., statistical analysis, biostatistics, computational analysis): C. Wang, M.S. Cicek, B. Charbonneau, K.R. Kalli, S.M. Armasu, M.C. Larson, G.E. Konecny, M.S. Block, D.W. Visscher, K.L. Knutson, B.L. Fridley, E.L. Goode

Writing, review, and/or revision of the manuscript: C. Wang, M.S. Cicek, B. Charbonneau, K.R. Kalli, S.M. Armasu, M.C. Larson, B. Winterhoff, J. Chien, V. Shridhar, M.S. Block, D.W. Visscher, J.M. Cunningham, K.L. Knutson, B.L. Fridley, E.L. Goode

Administrative, technical, or material support (i.e., reporting or organizing data, constructing databases): M.S. Cicek, M.C. Larson, J.-B. Fan, L.C. Hartmann, E.L. Goode

Study supervision: M.S. Cicek

Grant Support

This work was supported by the NIH (R01 CA122443 to E.L. Goode, P50-CA136393, Mayo Clinic SPORE in Ovarian Cancer to E.L. Goode, and R25 CA92049 to B. Charbonneau) and the Fred C. and Katherine B. Andersen Foundation (Women's Cancers: Improving Care through Genomics to E.L. Goode).

The costs of publication of this article were defrayed in part by the payment of page charges. This article must therefore be hereby marked *advertisement* in accordance with 18 U.S.C. Section 1734 solely to indicate this fact.

Received November 6, 2013; revised March 10, 2014; accepted March 24, 2014; published OnlineFirst April 11, 2014.

References

1. Siegel R, Naishadham D, Jemal A. Cancer statistics, 2013. CA Cancer J Clin 2013;63:11–30.
2. Koonings PP, Campbell K, Mishell DRJr, Grimes DA. Relative frequency of primary ovarian neoplasms: a 10-year review. Obstet Gynecol 1989;74:921–6.
3. Cicek MS, Koestler DC, Fridley BL, Kalli KR, Armasu SM, Larson MC, et al. Epigenome-wide ovarian cancer analysis identifies a methylation profile differentiating clear-cell histology with epigenetic silencing of the HERG K+ channel. Hum Mol Genet 2013;22:3038–47.
4. Shen H, Fridley BL, Song H, Lawrenson K, Cunningham JM, Ramus SJ, et al. Epigenetic analysis leads to identification of HNF1B as a subtype-specific susceptibility gene for ovarian cancer. Nat Commun 2013;4:1628.
5. Cancer Genome Atlas Research Network. Integrated genomic analyses of ovarian carcinoma. Nature 2011;474:609–15.
6. Bonome T, Levine DA, Shih J, Randonovich M, Pise-Masison CA, Bogomolniy F, et al. A gene signature predicting for survival in suboptimally debulked patients with ovarian cancer. Cancer Res 2008; 68:5478–86.
7. Tothill RW, Tinker AV, George J, Brown R, Fox SB, Lade S, et al. Novel molecular subtypes of serous and endometrioid ovarian cancer linked to clinical outcome. Clin Cancer Res 2008;14:5198–208.
8. Barton CA, Hacker NF, Clark SJ, O'Brien PM. DNA methylation changes in ovarian cancer: implications for early diagnosis, prognosis and treatment. Gynecol Oncol 2008;109:129–39.
9. Houshdaran S, Hawley S, Palmer C, Campan M, Olsen MN, Ventura AP, et al. DNA methylation profiles of ovarian epithelial carcinoma tumors and cell lines. PLoS One 2010;5:e9359.
10. Shih Ie M, Chen L, Wang CC, Gu J, Davidson B, Cope L, et al. Distinct DNA methylation profiles in ovarian serous neoplasms and their

Published OnlineFirst April 11, 2014; DOI: 10.1158/0008-5472.CAN-13-3198

implications in ovarian carcinogenesis. Am J Obstet Gynecol 2010; 203:584 e1–22.
11. Dai W, Teodoridis JM, Zeller C, Graham J, Hersey J, Flanagan JM, et al. Systematic CpG islands methylation profiling of genes in the Wnt pathway in epithelial ovarian cancer identifies biomarkers of progression-free survival. Clin Cancer Res 2011;17:4052–62.
12. Jones PA, Baylin SB. The epigenomics of cancer. Cell 2007;128: 683–92.
13. Bibikova M, Barnes B, Tsan C, Ho V, Klotzle B, Le JM, et al. High density DNA methylation array with single CpG site resolution. Genomics 2011;98:288–95.
14. Teschendorff AE, Marabita F, Lechner M, Bartlett T, Tegner J, Gomez-Cabrero D, et al. A beta-mixture quantile normalization method for correcting probe design bias in Illumina Infinium 450 k DNA methylation data. Bioinformatics 2013;29:189–96.
15. Koestler DC, Marsit CJ, Christensen BC, Karagas MR, Bueno R, Sugarbaker DJ, et al. Semi-supervised recursively partitioned mixture models for identifying cancer subtypes. Bioinformatics 2010;26: 2578–85.
16. Christensen BC, Smith AA, Zheng S, Koestler DC, Houseman EA, Marsit CJ, et al. DNA methylation, isocitrate dehydrogenase mutation, and survival in glioma. J Natl Cancer Inst 2011;103:143–53.
17. Pharoah PDP, Tsai Y-Y, Ramus SJ, Phelan CM, Goode EL, Lawrenson K, et al. GWAS meta-analysis and replication identifies three new susceptibility loci for ovarian cancer. Nat Genet 2013;45:362–70.
18. Tibshirani R, Hastie T, Narasimhan B, Chu G. Diagnosis of multiple cancer types by shrunken centroids of gene expression. Proc Natl Acad Sci U S A 2002;99:6567–72.
19. Chen YA, Lemire M, Choufani S, Butcher DT, Grafodatskaya D, Zanke BW, et al. Discovery of cross-reactive probes and polymorphic CpGs in the Illumina Infinium HumanMethylation450 microarray. Epigenetics 2013;8:203–9.
20. Bukur J, Jasinski S, Seliger B. The role of classical and non-classical HLA class I antigens in human tumors. Semin Cancer Biol 2012;22: 350–8.
21. Wei SH, Lin F, Wang X, Gao P, Zhang HZ. Prognostic significance of stathmin expression in correlation with metastasis and clinicopathological characteristics in human ovarian carcinoma. Acta Histochem 2008;110:59–65.
22. Curiel TJ, Coukos G, Zou L, Alvarez X, Cheng P, Mottram P, et al. Specific recruitment of regulatory T cells in ovarian carcinoma fosters immune privilege and predicts reduced survival. Nat Med 2004;10: 942–9.
23. Sato E, Olson SH, Ahn J, Bundy B, Nishikawa H, Qian F, et al. Intraepithelial CD8+ tumor-infiltrating lymphocytes and a high CD8+/regulatory T cell ratio are associated with favorable prognosis in ovarian cancer. Proc Natl Acad Sci U S A 2005;102:18538–43.
24. Gooden MJ, de Bock GH, Leffers N, Daemen T, Nijman HW. The prognostic influence of tumour-infiltrating lymphocytes in cancer: a systematic review with meta-analysis. Br J Cancer 2011;105:93–103.
25. Grivennikov SI, Karin M. Inflammatory cytokines in cancer: tumour necrosis factor and interleukin 6 take the stage. Ann Rheum Dis 2011;70 Suppl 1:i104–8.
26. Vitale M, Pelusi G, Taroni B, Gobbi G, Micheloni C, Rezzani R, et al. HLA class I antigen down-regulation in primary ovary carcinoma lesions: association with disease stage. Clin Cancer Res 2005;11: 67–72.
27. Han LY, Fletcher MS, Urbauer DL, Mueller P, Landen CN, Kamat AA, et al. HLA class I antigen processing machinery component expression and intratumoral T-cell infiltrate as independent prognostic markers in ovarian carcinoma. Clin Cancer Res 2008;14:3372–9.
28. Hwang W-T, Adams SF, Tahirovic E, Hagemann IS, Coukos G. Prognostic significance of tumor-infiltrating T cells in ovarian cancer: A meta-analysis. Gynecol Oncol 2012;124:192–8.
29. Dedeurwaerder S, Desmedt C, Calonne E, Singhal SK, Haibe-Kains B, Defrance M, et al. DNA methylation profiling reveals a predominant immune component in breast cancers. EMBO Mol Med 2011;3: 726–41.
30. Callahan MJ, Nagymanyoki Z, Bonome T, Johnson ME, Litkouhi B, Sullivan EH, et al. Increased HLA-DMB expression in the tumor epithelium is associated with increased CTL infiltration and improved prognosis in advanced-stage serous ovarian cancer. Clin Cancer Res 2008;14:7667–73.
31. Tamiolakis D, Kotini A, Venizelos J, Jivannakis T, Simopoulos C, Papadopoulos N. Prognostic significance of HLA-DR antigen in serous ovarian tumors. Clin Exp Med 2003;3:113–8.
32. Mora-Garcia Mde L, Duenas-Gonzalez A, Hernandez-Montes J, De la Cruz-Hernandez E, Perez-Cardenas E, Weiss-Steider B, et al. Up-regulation of HLA class-I antigen expression and antigen-specific CTL response in cervical cancer cells by the demethylating agent hydralazine and the histone deacetylase inhibitor valproic acid. J Transl Med 2006;4:55.
33. Setiadi AF, Omilusik K, David MD, Seipp RP, Hartikainen J, Gopaul R, et al. Epigenetic enhancement of antigen processing and presentation promotes immune recognition of tumors. Cancer Res 2008;68:9601–7.
34. Vitale M, Rezzani R, Rodella L, Zauli G, Grigolato P, Cadei M, et al. HLA class I antigen and transporter associated with antigen processing (TAP1 and TAP2) down-regulation in high-grade primary breast carcinoma lesions. Cancer Res 1998;58:737–42.
35. Kaklamanis L, Leek R, Koukourakis M, Gatter KC, Harris AL. Loss of transporter in antigen processing 1 transport protein and major histocompatibility complex class I molecules in metastatic versus primary breast cancer. Cancer Res 1995;55:5191–4.

Published OnlineFirst April 11, 2014; DOI: 10.1158/0008-5472.CAN-13-3198

Cancer Research
The Journal of Cancer Research (1916–1930) | The American Journal of Cancer (1931–1940)

AACR American Association for Cancer Research

Tumor Hypomethylation at 6p21.3 Associates with Longer Time to Recurrence of High-Grade Serous Epithelial Ovarian Cancer

Chen Wang, Mine S. Cicek, Bridget Charbonneau, et al.

Cancer Res 2014;74:3084-3091. Published OnlineFirst April 11, 2014.